

# Semiconductor Optical Active Devices for Photonic Networks

●Kiyohide Wakao ●Haruhisa Soda ●Yuji Kotaki

*(Manuscript received January 28, 1999)*

**This paper describes recent progress in semiconductor optical active devices for photonic networks. The characteristics of modulator-integrated distributed feedback lasers, tapered-thickness waveguide lasers, and semiconductor optical amplifiers are improved by introducing a strained-layer into the active regions. Experimental results show that these devices are promising for photonic networks.**

## 1. Introduction

Semiconductor optical active devices are the key components for photonic networks such as wavelength division multiplexing (WDM) systems and access systems. Over the past 10 years, great progress has been made with semiconductor optical active devices by developing three technologies. The first is a technology for monolithic integration of a laser with another optical component. This has enabled us to realize low-chirp modulator-integrated distributed feedback (MI-DFB) lasers and tapered-thickness waveguide lasers which can be satisfactorily coupled to a single mode fiber without needing a lens, thereby enabling the construction of extremely low-cost optical modules. The second technology is a strained-layer active material, which has brought excellent lasing characteristics such as low-threshold, high-efficiency operation of semiconductor lasers due to 'band engineering' of a semiconductor material.<sup>1-3)</sup> The third is a metal-organic vapor phase epitaxial (MOVPE) technology. This growth technology has made it possible not only to obtain the high-quality strained-layer quantum wells necessary for improving the lasing characteristics mentioned above, but also to fabricate new types

of planar buried-heterostructures (BHs) with Fe-doped semi-insulating current blocking layers and p-n junction current blocking. Such buried-heterostructures have shown high-speed operation and high-temperature operation because of low parasitic capacitance and good current confinement. These three technologies make semiconductor optical active devices such as MI-DFB lasers and tapered-thickness waveguide lasers promising components for photonic networks.

This paper describes recent progress that has been made with MI-DFB lasers, tapered-thickness waveguide lasers, and semiconductor optical amplifiers (SOA). All these devices have strained-layer active regions and are fabricated using all-MOVPE growth. They exhibit high-performance device characteristics.

## 2. Modulator-integrated DFB lasers

MI-DFB lasers are attractive candidates for the light sources of WDM systems. The structure of an MI-DFB laser is shown in **Figure 1**. It consists of a DFB laser and an electro-absorption optical modulator. These two elements are monolithically integrated using a butt-joint scheme. The lasing characteristics of the MI-DFB laser are

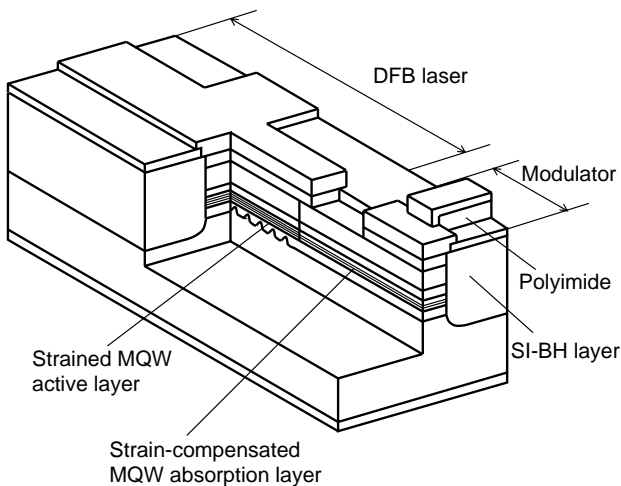


Figure 1  
Structure of MI-DFB laser.

mostly determined by the performance of the modulator. We have developed a new type of a modulator which has a strain-compensated structure with a combination of InGaAsP compressive wells and InGaAsP tensile barriers. This strain-compensated structure is superior in frequency response to the conventional non-strained quantum wells because the strain-compensated structure forms shallow wells in the valence band, which reduces the hole escape time from the wells.<sup>2),3)</sup> Therefore, higher-speed operation can be achieved with this structure. The strain-compensated structure also provides deep wells in the conduction band. This increases the absorption coefficient due to the large overlap integral of wave functions between electrons and holes, and makes the modulator operate at a lower voltage. Thus, the introduction of a strained-layer into the modulator improves its performance.

We fabricated the MI-DFB lasers using a five-step all-MOVPE growth technique. The buried-heterostructure with semi-insulating current blocking layers was used to reduce the parasitic capacitance of the modulator. Details about the fabrication process are described in reference 4). The lengths of the DFB laser and the modulator were 300  $\mu\text{m}$  and 200  $\mu\text{m}$ , respectively.

The threshold current of the DFB laser was

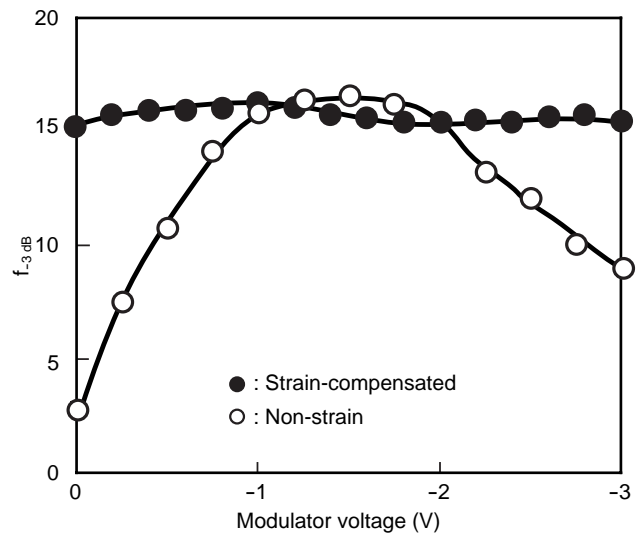


Figure 2  
-3 dB bandwidth of MI-DFB laser. Black circles are the results for MI-DFB laser with strain-compensated absorption layer and white circles are for laser with non-strained absorption layer.

5.5 mA. The maximum optical output power of 24 mW was obtained with an injection current of 150 mA. The extinction ratio was 13 dB when the modulator was biased from 0 to -2 V. The lasing wavelength was 1.554  $\mu\text{m}$ .

The modulation bandwidth was measured by the small signal response. **Figure 2** shows the dependence of the -3 dB bandwidth on modulator voltage. A bandwidth higher than 15 GHz was obtained over the entire modulator bias range. These characteristics were better than those of the conventional MI-DFB lasers with non-strained quantum wells in the modulator. The results showed that hole carriers were completely swept out from the wells of the valence band. This was true even with a low modulator voltage (when the electric field applied to the wells was weak) and with a high modulator voltage (when many hole carriers were generated in the wells due to the large absorption coefficient of the wells).

MI-DFB lasers exhibit chirping in dynamic modulation. In chirping, the lasing wavelength moves to the shorter-wavelength side (blue-chirp) or to the longer-wavelength side (red-chirp) as the amplitude of the output light is modulated. The

blue-chirp characteristics are attractive in light transmission using a conventional single-mode fiber because, at the beginning of the transmission, the blue-chirp can suppress light pulse broadening due to the dispersion of the fiber, which is the most dominant limiter of the transmission distance. These blue- and red-chirp characteristics are defined by the chirp parameter  $\alpha$  and depend on the structure of the device and the modulator voltage. **Figure 3** shows the dependence of  $\alpha$  on the modulator voltage. As can be seen,  $\alpha$  became negative (blue-chirp) at a high modulator bias. The modulator voltage for  $\alpha = 0$  was smaller in the strain-compensated lasers than in the conventional MI-DFB lasers. This is because hole accumulation causes field screening in the modulator of conventional MI-DFB lasers. Therefore, the strain-compensated MI-DFB lasers have superior long-distance transmission characteristics.

Next, we examined the 10 Gb/s NRZ transmission characteristics using a standard single-mode fiber with a dispersion of 17 ps/nm/km at 1.55  $\mu\text{m}$ . The modulator bias was set at 2.0 V. The bit error rate (BER) curves before and after transmission over 100 km are shown in **Figure 4**. No appreciable power penalty was seen

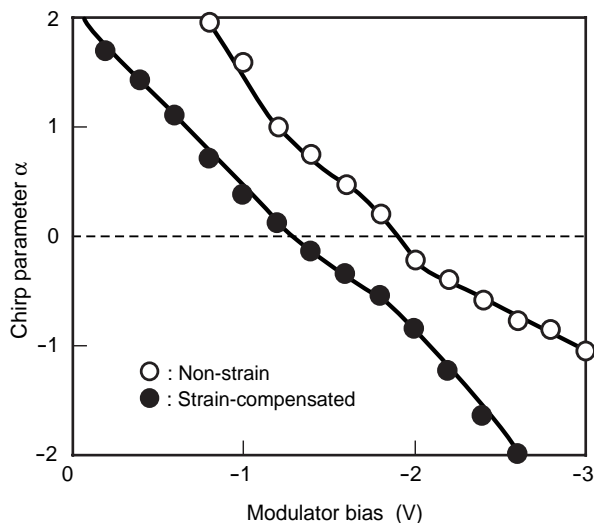


Figure 3 Chirp parameter dependence on modulator bias voltage.

at a BER of  $10^{-11}$ . This agreed with the finding that transient blue chirp was clearly observed in time-resolved dynamic chirp measurement using a fiber interferometer.

These results indicate that the MI-DFB lasers are promising as blue-chirp light sources in multi-gigabit photonic networks.

### 3. Tapered-thickness waveguide lasers

The reduction of the cost of optical modules is one of the most important requirements for realizing optical access systems. From this viewpoint, light sources must have a narrow beam divergence and be able to operate without the need for coolers or automatic-power-control (APC). Tapered-thickness waveguide lasers are promising light sources for optical access systems because the optical coupling between the laser and fiber can be done directly without a lens. Thus, we

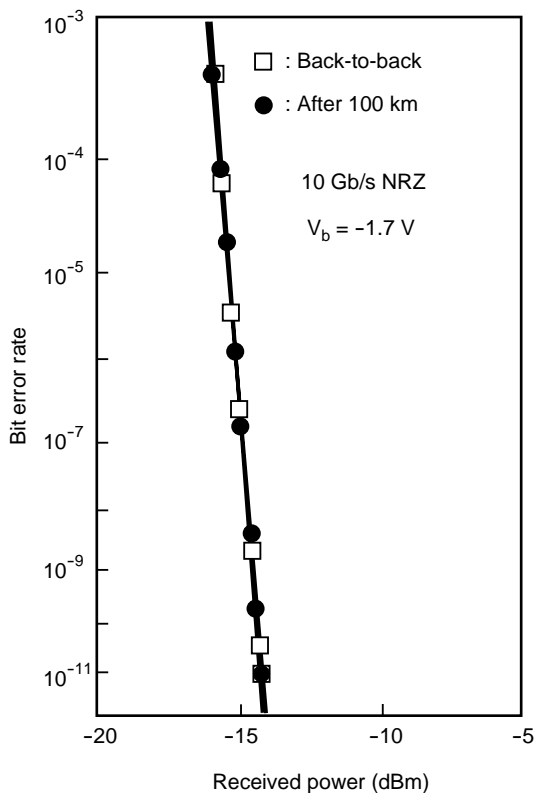


Figure 4 Bit error rate characteristics of 100 km transmission experiments.

examined the possibility of achieving these cost-reducing requirements in tapered-thickness waveguide lasers.

The schematic structure of the tapered-thickness waveguide laser is shown in **Figure 5**. The laser has a uniform-thickness active region and a tapered-thickness passive region, where the spot size of the guided mode expands as the light propagates to the front facet. Due to the spot size converter, a narrow beam divergence is realized and good optical coupling between the laser and fiber is attained without using a lens. A compressive strained-layer is used in the active region to obtain a low threshold and high-efficiency operation.

The lasers were fabricated using three-step all-MOVPE growth. The tapered-thickness configuration was obtained by selective MOVPE growth.<sup>5,6)</sup> The buried-heterostructure with p-n junction current blocking layers was made using a dry-etching process and MOVPE with CH<sub>3</sub>Cl gas addition.<sup>7)</sup> By adding CH<sub>3</sub>Cl gas in the burying growth, planar BH structures were realized. The lasers were 500 μm long.

**Figure 6** shows the light output versus current characteristics of the tapered-thickness

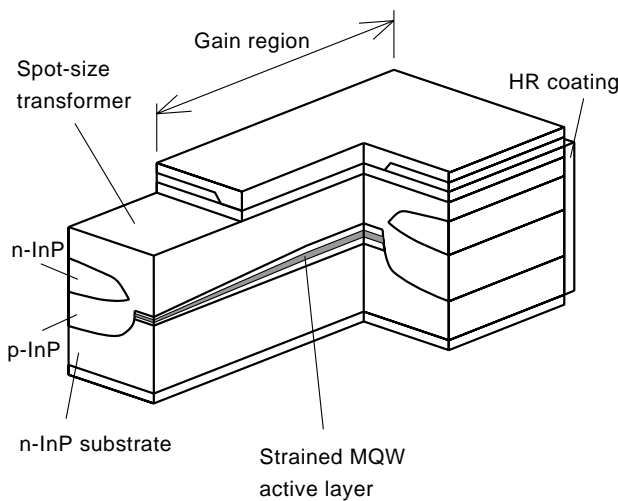


Figure 5  
Structure of tapered-thickness waveguide laser.

waveguide laser. The threshold currents were 6.0 mA at 25°C, 19.0 mA at 85°C, and 27.7 mA at 100°C. A low operating current of 48.5 mA for a 10 mW output power at 85°C was achieved, and an output power of over 20 mW was obtained up to 100°C. These values are the best among the lasers fabricated using three-step MOVPE growth. The far-field patterns of the laser were 9° in the horizontal axis and 10° in the vertical axis. A coupling efficiency of -2.3 dB was obtained with direct coupling to a single-mode fiber without a lens.

Transmission experiments were carried out using 40 km of standard single-mode fiber. We used a tapered-thickness waveguide laser with p-n current blocking layers grown by liquid phase epitaxy.<sup>5)</sup> The laser was biased at 1 mA and modulated at 155.52 Mb/s NRZ with an external optical feedback of -14 dB. Penalty-free transmission was achieved at 85°C, as shown in **Figure 7**. We found that optical feedback of up to -14 dB did not cause any power penalty. These results show that the narrow beam divergence lasers are suitable for isolator-free, coolerless, fixed-bias, APC-free transmission.

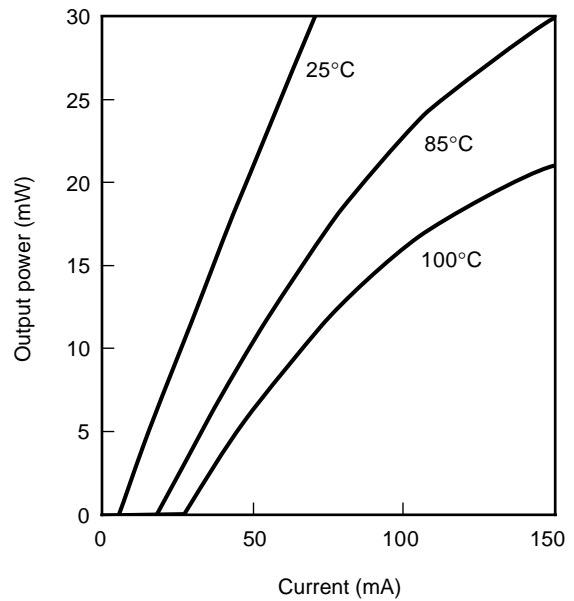


Figure 6  
Light output power versus current characteristics. The lasing wavelength was 1.31 μm.

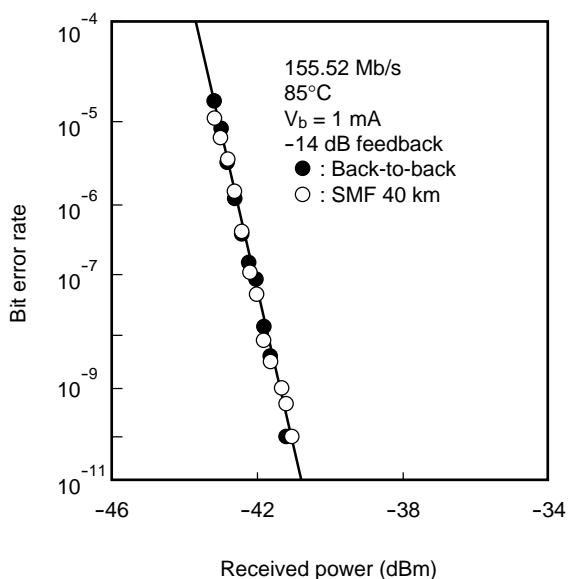


Figure 7 Bit error rate characteristics of 40 km transmission experiments. The laser was biased at 1 mA at 85°C with optical feedback of -14 dB.

#### 4. Semiconductor optical amplifiers

Semiconductor optical amplifiers are being considered for applications in photonic networks because of their high-gain, wide-bandwidth, compactness, and monolithic integrability with other semiconductor devices. The structure of the SOA is shown in **Figure 8**. The active layer is tensile-strained thick InGaAsP that is 0.2 μm thick and 1.0 μm wide. The use of tensile strain, which gives a larger optical gain for light having a transverse magnetic (TM) polarization is an effective way to compensate for the polarization sensitivity of rectangular-shaped active waveguides, which is due to the larger optical confinement in the active layer for transverse electric (TE) polarization than for TM polarization. Thus, we can realize polarization insensitive SOAs with wide active regions, which are most commonly used in conventional semiconductor lasers.

The fabrication process of the SOAs was very similar to that of lasers. The mesa stripes were made by a dry-etching process, then they were buried using selective MOVPE growth. The dif-

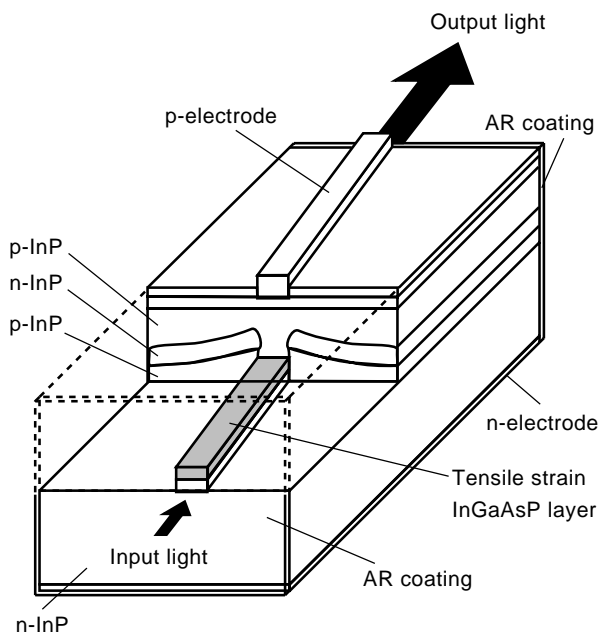


Figure 8 Structure of semiconductor optical amplifier. The active stripe is slanted by 7° from the <011> direction. Both facets are coated with anti-reflection films.

ference here is that the mesa stripes were formed 7° off from the <011> direction to prevent the gain from having a resonant peak due to the formation of an optical cavity. The length of the SOAs was 600 μm. Anti-reflective films were coated on both facets.

**Figure 9** shows the gain characteristics of the SOA for the TE and TM modes. The fiber-to-fiber gain became positive at around a current of 55 mA, and a gain exceeding 12 dB was obtained at 100 mA. The optical coupling loss between the SOA and the fibers was about 6dB per facet, so the internal optical gain of the SOA was estimated to be as high as 24 dB. A polarization insensitivity of less than 1 dB was attained over the current range from 50 to 100 mA. This indicates that the polarization dependence was well-compensated for by the tensile strain of the active layer. These characteristics make this SOA attractive as a loss-compensation optical amplifier. In addition, a large on/off ratio of more than 70 dB was attained for injection currents of 10 mA and 100 mA. Such a large extinction is at-

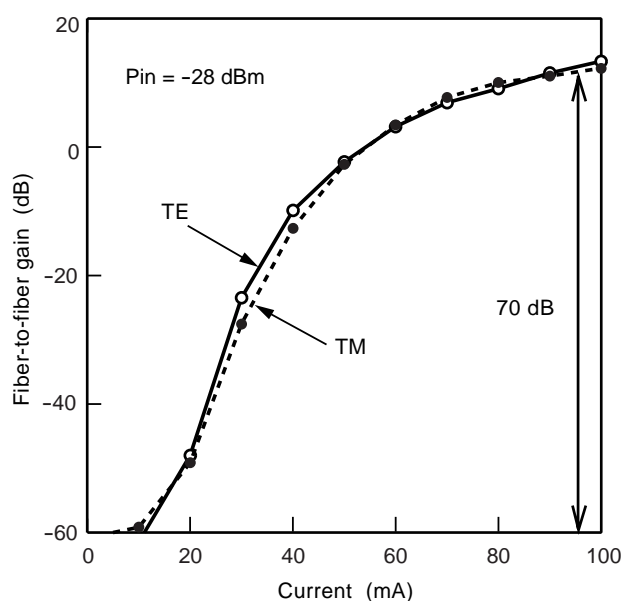


Figure 9  
Fiber-to-fiber gain versus current characteristics for measured incident light of -28 dBm and 1.55  $\mu\text{m}$ .

tractive for use in an optical switch such as the one shown in **Figure 10** because extremely low cross-talk is realized with this configuration when the SOA is used as an optical gate.

## 5. Conclusion

This paper discussed recent progress that has been made with modulator-integrated distributed feedback lasers, tapered-thickness waveguide lasers, and semiconductor optical amplifiers. The characteristics of these devices were improved by introducing a strained-layer into the active regions. MI-DFB lasers with a strained-compensated modulator exhibited blue-chirp characteristics, and 10 Gb/s, 100 km transmission experiments were successfully performed. The tapered-thickness waveguide lasers were fabricated using all-MOVEP growth and a dry-etching process. A low threshold operation of 6 mA was attained at room temperature, and a high output power of 20 mW was attained at 100°C. Polarization insensitive SOAs were realized using a tensile active layer, and a high gain of more than 24 dB and a large extinction ratio of 70 dB were obtained. These

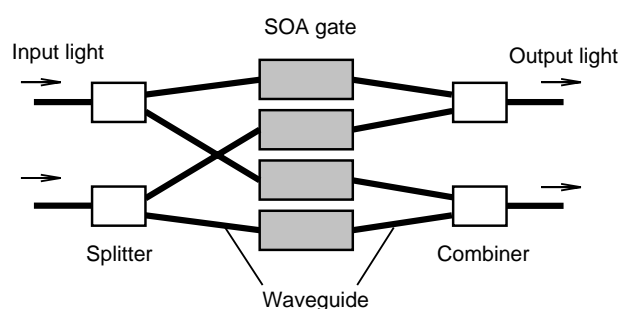


Figure 10  
2  $\times$  2 optical switch using SOA gates. Here, the SOAs are used as optical gates and as optical amplifiers.

characteristics show that the device is promising as a key component for photonic networks.

## References

- 1) E. Yablonovitch and E. O. Kane: Reduction of Lasing Threshold Current Density by the Lowering of Valence Band Effective Mass. *J. Lightwave Technol.*, **LT-4**, 5, pp.504-506 (1986).
- 2) R. Sahara, K. Morito, and H. Soda: Engineering of Barrier Band Structure for Electro-absorption MQW Modulators. *Electron. Lett.*, **30**, 9, pp.698-699 (1994).
- 3) I. K. Czajkowski, M. A. Gibbon, G. H. B. Thompson, P. D. Greene, A. D. Smith, and M. Silver: Strained-compensated MQW electro-absorption Modulator for Increased Optical Power Handling. *Electron. Lett.*, **30**, 11, pp.900-901 (1994).
- 4) K. Morito, R. Sahara, K. Sato, Y. Kotaki, and H. Soda: High Power Modulator Integrated DFB Laser Incorporating Strain-Compensated MQW and Graded SCH Modulator for 10 Gbit/s. *Electron. Lett.*, **31**, 12, pp.975-976 (1995).
- 5) H. Kobayashi, T. Yamamoto, M. Ekawa, T. Watanabe, T. Ishikawa, T. Fujii, H. Soda, S. Ogita, and M. Kobayashi: Narrow-Beam Divergence 1.3- $\mu\text{m}$  Multiple-Quantum-Well Laser Diodes With Monolithically Integrat-

ed Tapered Thickness Waveguide. *IEEE J. Select. Topics in Quantum Electron.*, **3**, 6, pp.1384-1389 (1997).

- 6) T. Yamamoto, H. Kobayashi, M. Ekawa, T. Fujii, H. Soda, and M. Kobayashi: High Temperature Operation of 1.3- $\mu$ m Narrow Beam Divergence Tapered Thickness Waveguide

BH Lasers. *Electron. Lett.*, **31**, 25, pp.2178-2179 (1995).

- 7) T. Takeuchi, and S. Yamazaki: Planar InP Burying Growth around a Dry-Etched Mesa by Addition of CH<sub>3</sub>Cl during MOVPE. Seventh Int. Conf. on Indium Phosphide and Related Materials, Sapporo, Japan, 1995, May, WP56, pp.291-294.



**Kiyohide Wakao** received the B.E. and Ph.D degrees in Electronics Engineering from Tokyo Institute of Technology, Tokyo, Japan in 1976 and 1981, respectively. He joined Fujitsu Laboratories Ltd., Kawasaki in 1981 and has been engaged in the research and development of InGaAsP/InP lasers, semiconductor optical functional devices, and CMOS analog circuits for optical communications. He is a member of the

Japan Society of Applied Physics and the Institute of Electronics, Information and Communication Engineers (IEICE) of Japan.

E-mail : kwakao@flab.fujitsu.co.jp



**Yuji Kotaki** received the B.E. and M.E. degrees in Electronics Engineering from Tokyo Institute of Technology, Tokyo, Japan in 1982 and 1984, respectively. He joined Fujitsu Laboratories Ltd., Kawasaki in 1984 and has been engaged in the research and development of semiconductor lasers for optical fiber transmission systems.

E-mail : ykotaki@flab.fujitsu.co.jp



**Haruhisa Soda** received the B.E., M.E., and Ph.D. degrees in Electronics Engineering from Tokyo Institute of Technology, Tokyo, Japan in 1978, 1980, and 1983, respectively. He joined Fujitsu Laboratories Ltd., Kawasaki in 1983. He is now a senior researcher of the Optical Semiconductor Devices Laboratory.

E-mail : soda@flab.fujitsu.co.jp